

Development of a Boundary Layer Property Interpolation Tool in Support of Orbiter Return To Flight

Francis A. Greene*

NASA Langley Research Center, Hampton, VA 23681

H. Harris Hamilton†

North Carolina State University, Raleigh, NC 27695

A new tool was developed to predict the boundary layer quantities required by several physics-based predictive/analytic methods that assess damaged Orbiter tile. This new tool, the Boundary Layer Property Prediction (BLPROP) tool, supplies boundary layer values used in correlations that determine boundary layer transition onset and surface heating-rate augmentation/attenuation factors inside tile gouges (i.e. cavities). BLPROP interpolates through a database of computed solutions and provides boundary layer and wall data (δ , θ , Re_θ , M_e , Re_θ/M_e , Re_θ , P_w , and q_w) based on user input surface location and free stream conditions. Surface locations are limited to the Orbiter's windward surface. Constructed using predictions from an inviscid w/ boundary-layer method and benchmark viscous CFD, the computed database covers the hypersonic continuum flight regime based on two reference flight trajectories. First-order one-dimensional Lagrange interpolation accounts for Mach number and angle-of-attack variations, whereas non-dimensional normalization accounts for differences between the reference and input Reynolds number. Employing the same computational methods used to construct the database, solutions at other trajectory points taken from previous STS flights were computed: these results validate the BLPROP algorithm. Percentage differences between interpolated and computed values are presented and are used to establish the level of uncertainty of the new tool.

Nomenclature

h, H	= Enthalpy, lbm/ft^2	Subscripts
M	= Mach number	e = Boundary layer edge
P	= surface pressure, lbs/ft^2	o = Total conditions
q	= surface heating-rate, $\text{BTU/ft}^2\text{-s}$	w = Wall
Re	= Unit Reynolds number, $1/\text{ft}$	∞ = Free Stream
Re_θ	= momentum thickness Reynolds number	
Re_θ/M_e	= transition parameter	
T	= Temperature, R	
T_v	= Vibrational temperature, R	
s, β, n	= streamline coordinates	
V	= Velocity, ft/s	
x_s	= damage coordinate – axial, in	
y_s	= damage coordinate – vertical, in	
z_s	= damage coordinate – lateral, in	
α	= angle-of-attack, deg	
δ	= boundary layer thickness, in	
θ	= momentum thickness, in	
ρ	= density, slug/ft^3	

* Aerospace Technologist, Aero-Thermodynamics Branch, Mail Stop 408A, Senior Member.

† Visiting Researcher, Aero-Thermodynamics Branch, Mail Stop 408A

I. Introduction

Teams of researchers developed a suite of physics-based predictive/analytic tools¹ that assess the need to repair damaged thermal protection system (TPS) tiles on the Shuttle Orbiter. Damage can be in the form of either a cavity or a protuberance. Development of these tools was in direct alignment with several Columbia Accident Investigation Board (CAIB)² recommendations. During entry, the Orbiter may experience a deviation from its nominal surface heating-rate and/or heat-load profile if there is extensive damage to the TPS tile. Higher than nominal heat-load or excessive surface temperature can over stress the TPS, thus compromising Orbiter survivability. Therefore, the consequences of an abnormal aero-heating environment have to be examined to make fly as is, no-fly, or repair recommendations. Recommendations are based on an integrated analysis from a collection of tools that estimate the Orbiter's external aero-thermal and structural environment. Figure 1. is a simple illustration showing how these tools interact.

The boundary layer transition (BLT) and cavity heating tools (highlighted in red in Figure 1) are two components that contribute to defining the Orbiter's external aero-thermal and structural environment. Based on recently obtained experimental³ data incorporated within an existing methodology^{4,5,6}, the BLT tool⁷ predicts whether transition will occur and if so estimates the onset time. The BLT tool requires boundary layer thickness (δ) and transition parameter (Re_{θ}/M_e) to estimate transition onset times associated with cavity and protuberance damage. The Cavity Heating tool estimates the surface heating-rate augmentation/attenuation factors inside a cavity. The heating-rate bump factors are derived from correlations that require boundary layer thickness and edge Mach number (M_e). Both the BLT and Cavity Heating analysis tools aid in the estimation of the external environment and support the structural thermal analysis. Boundary layer transition from an experimental³ and flight perspective^{8,9}, and an overview of the cavity heating¹ methodology are discussed in companion papers.

In response to the requirement for boundary layer data through the entire hypersonic continuum flight regime, a computational tool that automates the process of generating this data was developed. The new tool, the Boundary Layer Property Prediction (BLPROP) tool, feeds data to the BLT and Cavity Heating analysis tools. Through its interaction with these two tools, BLPROP contributes to the analysis from both a localized and acreage perspective; therefore, it has a significant roll in TPS damage scenarios. For every future shuttle mission if damage is identified, the process in Figure 1 will be exercised. During the STS-114 Return to Flight (RTF) mission, damage in the form of protruding gap fillers was identified. BLPROP supplied the boundary layer edge values needed for RTF pre-mission and on-mission analysis; this includes the analysis used to support a decision to perform an unplanned EVA to remove the two protruding gap fillers (Ref. 8). While the current application is for Orbiter mission support, BLPROP can be used on any vehicle upon which a suitable database is available.

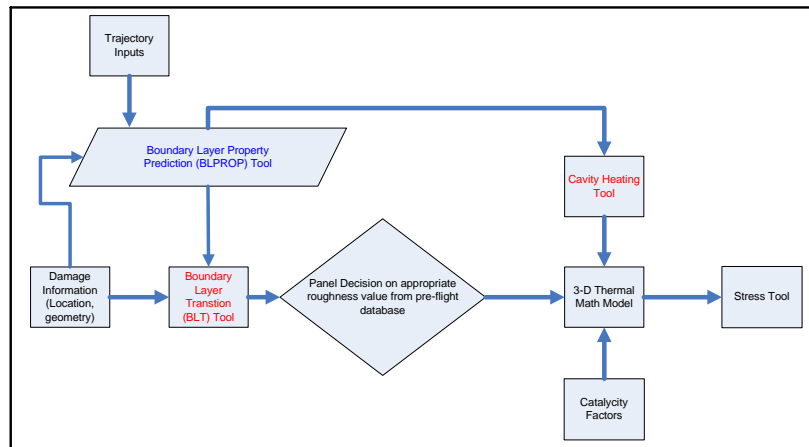


Figure 1. Aero-heating Tool Flow Diagram

A brief description of BLPROP follows. Written to be self-contained and function without user intervention other than specifying damage location and free stream conditions, BLPROP consists of a database of computed solutions, a main routine that loads the database and outputs values, and a few subroutines that perform computations. The algorithm, coded in FORTRAN 77 and designed to be incorporated within existing software, functions in any big endian computing environment. BLPROP interpolates through the database to provide boundary layer and surface data at user specified input conditions. Given the possibility of early boundary layer transition and

that the highest nominal heating-rates are on the windward surface, damage assessment is limited to the Orbiter's windward surface. Within BLPROP is a geometry-based search algorithm that determines the mesh index pair in the database domain nearest to the damage location. A first-order one-dimensional Lagrange interpolation method determines values at the input angle-of-attack and Mach number, whereas non-dimensional normalization accounts for the differences between the reference and input Reynolds number. The database covers the hypersonic continuum flight regime and is based on two reference trajectories (ISSHVFW & reconstructed STS-107); this rationale is explained in the next section. The ISSHVFW trajectory is a fictitious heavy weight return flight from the International Space Station and STS-107 is the reconstructed Columbia Orbiter trajectory. An inviscid w/ boundary-layer computational method and benchmark viscous CFD solvers populated the database along the ISSHVFW and STS-107 trajectories, respectively. Interpolated values from BLPROP and computed data from higher fidelity methods are presented, along with a description of the BLPROP methodology and database.

II. Database Description

This section describes computational database in BLPROP. Variables in the database are surface pressure, heating-rate, momentum thickness, **boundary layer thickness**, non-dimensional edge velocity components, **edge Mach number**, and **transition parameter (Re_{θ}/M_e)**. While the analysis tools BLPROP support require only those variables in bold type, it is not unlikely that other applications or modification to supported tools would require the remaining variables, hence their inclusion. Database values exist at ordered discrete coordinate locations on the Orbiter's windward surface. The computational database does not contain volume or flow field information. The database mesh contains 101 axial and 56 lateral points with a small portion of the nose cap and wing leading edge not represented. Initially, data resided on the mesh utilized by one of the computational methods listed in the next paragraph. This original data was transferred to the database mesh using the inverse distance interpolation option in Tecplot®. Thus, each database solution resides on the same mesh. Interpolation with a Kriging method yielded spurious results, hence the selection of the inverse distance method.

Three computational methods, LAURA¹⁰ (Langley Aerothermodynamic Upwind Relaxation Algorithm), DPLR¹¹ (Data-Parallel Line Relaxation), and LATCH¹² (Langley Approximate Three-Dimensional Convective Heating) provide the database foundation. LAURA and DPLR are viscous benchmark CFD solvers, whereas LATCH is an engineering method that requires an inviscid solution: all inviscid solutions were computed using the LAURA code. Depending on the Mach number, LATCH solutions assumed either equilibrium or perfect gas chemistry. In addition, LAURA and DPLR used a 5-species non-equilibrium chemistry model and a finite catalytic recombination model. All data computed were at laminar conditions and assumed a radiation equilibrium wall condition. The next section describes each computational method in more detail.

Methods of defining the boundary layer edge differ between LATCH and viscous CFD approaches. Because LATCH is based on an inviscid solution, a viscous layer doesn't exist. LATCH edge values are theoretical, evaluated from correlations, or taken directly from the inviscid solution. LATCH computes a momentum thickness and determines boundary layer thickness using a shape-factor ($\delta/\theta=C$). For air test facilities that are part of the Langley Aerothermodynamic Laboratory, C is 7.5, while at flight conditions C varies with $h_w/(H_o)_{\infty}$. Edge velocities and surface pressure come directly from the wall of the inviscid solution. The laminar-heating rate is computed from an equation that relates heating rate to the momentum thickness Reynolds number. Viscous CFD solutions have a viscous layer and require an interrogation of the flow field to determine edge values. In this work, an algorithm developed during RTF activities, BLAYER_RESULTS¹³, interrogated LAURA and DPLR solutions to define a boundary layer edge and determine edge values. In BLAYER_RESULTS, detection of the boundary layer edge is based on a total enthalpy ratio. Rather than using the conventional criterion (99.5% of total enthalpy ratio) to define the boundary layer edge, BLAYER_RESULTS utilizes a maximum curvature specification of the total enthalpy profile to define the boundary layer edge. The primary motivation for using a maximum curvature approach in place of the 99.5% method is that numerical losses through a strong bow shock are different for different streamlines. Thus, the total enthalpy in the CFD solutions at flight conditions is seen to vary in the inviscid portion of the flow behind the shock in a non-physical way due to differences in numerical dissipation. This can cause the conventional edge detection method to inaccurately locate the boundary layer edge. With the edge defined, BLAYER_RESULTS interpolates along grid lines to determine edge values.

Free stream conditions for the database are taken from two trajectories: the STS-107 trajectory from Mach 25.7 to 22.9 and the ISSHVFW trajectory from Mach 20.3 to 6.0. These trajectories have very similar Mach number-Reynolds number profiles. The ISSHVFW data, computed using the two-layer approach, and the STS-107 data,

computed using the viscous CFD solvers, cover the hypersonic flight regime. Initially developed only for BLT analysis, the BLPROP database consisted solely of two-layer data. Incorporating the STS-107 data was a subsequent addition to the database to cover the Mach number range required for cavity heating analysis. Because two-layer data did not exist at the Mach number range covered by the STS-107 data, a programmatic decision was made to use the pre-existing STS-107 solutions. This mixing of computational methods presents some inconsistencies that were accepted as risks. Experience with boundary layer transition correlations indicates the same computational method should be used for correlation development and application at flight. The BLT correlation was developed using two-layer data; therefore, the correlation must use two-layer data when evaluated for flight. The inconsistency for the BLT analysis is at the upper Mach numbers covered by the STS-107 data. Cavity Heating correlations were developed based on viscous CFD. Therefore, the inconsistency is reversed, existing at the Mach range covered by the two-layer data. Efforts to resolve database conflicts are in progress. An all viscous CFD database has since been generated and work is in progress to incorporate it an updated version of BLPROP. In addition, viscous based boundary layer transitions correlations are under study.

Figure 2 is an illustration of the Mach number versus angle-of-attack space covered by the database. Each filled symbol represents a solution in the database. A total of 42 solutions cover the entry trajectory corridor. Existing STS-107 CFD data, Orbiter GN&C angle-of-attack limits, a requirement to cover the hypersonic continuum flight regime, and angle-of-attack history from previous Shuttle flights were the basis for point selection. Data points at each Mach number surround the angle of attack bounds from previous shuttle flights¹⁴ and the GN&C limits from the Shuttle Operational Data Book (SODB)¹⁵. This ensures data interpolation, rather than extrapolation, as a function of angle-of-attack. It also enables the BLPROP tool to provide data at any angle of attack along a trajectory within the bounds of the points shown. The angle of attack bounds are:

Mach 6.0 → 8.0	$\alpha = 20 \rightarrow 40$
Mach 8.0 → 10.0	$\alpha = 30 \rightarrow 45$
Mach 10.0 → 25.7	$\alpha = 35 \rightarrow 45$

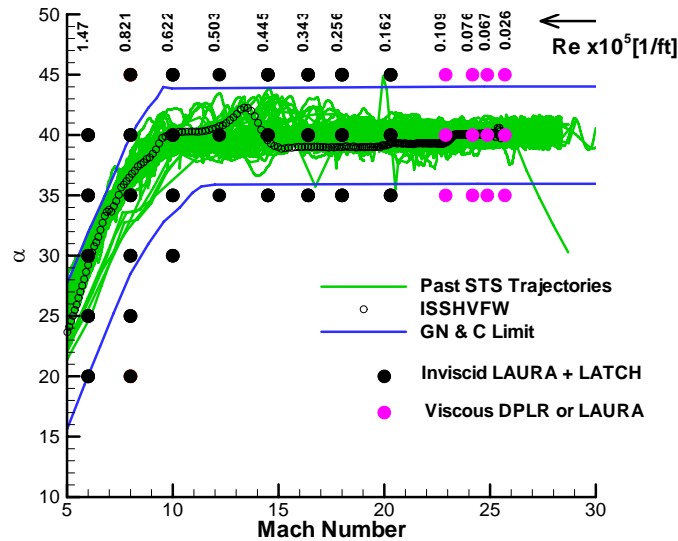


Figure 2. BLPROP database - Mach number vs. angle-of-attack

At the lower and higher Mach numbers time intervals are 1 and approximately 2 minutes, respectively. The free stream reference conditions for solutions in the database follow:

Table 1. STS-107 Flight Trajectory (reconstructed) Free Stream Conditions

Time past EI, s	M_∞	T_∞ , R	V_∞ , ft/s	ρ_∞ , slug/ft ³	α , deg	Chemistry/Code
t=305	25.7	380	24603	3.314×10^{-8}	35, 41.35, 45	5-sp NEQAir/LAURA
t=415	24.9	391	24116	7.568×10^{-8}	35, 40.17, 45	5-sp NEQAir/DPLR
t=500	24.2	395	23554	1.017×10^{-7}	35, 39.99, 45	5-sp NEQAir/DPLR
t=625	22.9	401	22504	1.5518×10^{-7}	35, 39.59, 45	5-sp NEQAir/DPLR

Table 2. ISSHVFW Flight Trajectory Free Stream Conditions

Time past EI, s	M_∞	T_∞ , R	V_∞ , ft/s	ρ_∞ , slug/ft ³	α , deg	Chemistry/Code
790	20.3	421	20475	2.557×10^{-7}	35, 40, 45	EQAir/LATCH
900	18.0	433	18368	4.598×10^{-7}	35, 40, 45	EQAir/LATCH
970	16.4	444	16960	6.804×10^{-7}	35, 40, 45	EQAir/LATCH
1030	14.5	457	15192	1.008×10^{-6}	35, 40, 45	EQAir/LATCH
1100	12.2	464	12904	1.356×10^{-6}	35, 40, 45	EQAir/LATCH
1170	10.0	472	10623	2.068×10^{-6}	30, 35, 40, 45	EQAir/LATCH
1240	8.0	471	8454	3.425×10^{-6}	20, 25, 30, 35, 40, 45	PGAir/LATCH
1330	6.0	448	6030	7.995×10^{-6}	20, 25, 30, 35, 40	PGAir/LATCH

III. Computational Methods

A. LATCH

This section gives a summary description of the Langley Approximate Three-Dimensional Convective Heating (LATCH) code¹⁶. A complete description of LATCH is in Refs. 16 and 17. LATCH is an approximate three-dimensional heating code based on the axisymmetric analog for general three-dimensional boundary layers¹⁸. The boundary-layer equations are written in a streamline-oriented coordinate system (s, β, n) , where s is the distance measured along an inviscid streamline, β is tangent to the surface and normal to the streamline direction, and n is normal to the surface (see Figure 3). If the viscous cross-flow in the boundary-layer is small and can be neglected (as it can be when the streamline curvature is small or the wall is cold), the boundary-layer equations reduce to an axisymmetric form if s is interpreted as the distance along an "equivalent" axisymmetric body and the metric coefficient h , associated with the spreading of the streamlines, is interpreted as the radius of the equivalent axisymmetric body. This assumption allows the calculation of approximate three-dimensional heating rates along individual streamlines, independent of other streamlines, using any axisymmetric heating prediction method. The approach is simplified further by using an approximate integral heating technique¹⁹, which has been shown to agree with more detailed finite-difference boundary-layer solutions for heating rates. Using this approach LATCH calculates, assuming either perfect gas or equilibrium air, laminar or turbulent heating rates on re-entry vehicles along individual streamlines. A large number of streamlines are computed simultaneously starting immediately downstream of the nose region; then, at each new computational step down the body, the streamlines are redistributed to achieve a more uniform distribution around the body. Thus, the heating over the entire body can be computed in a single pass with no user intervention. At flight conditions, LATCH predicts wall temperatures using a radiation equilibrium condition similar to that shown in equation (1) below.

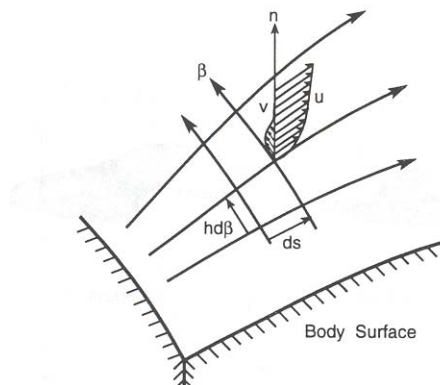


Figure 3. Typical surface streamline and boundary layer profile

The calculation of reasonably accurate heating rates in significantly less time than what is required for a benchmark Navier-Stokes code is the primary advantage of LATCH. While LATCH requires an inviscid solution, the computational time required for an inviscid solution is an order of magnitude less than for a viscous solution. LATCH itself requires only 1-5 minutes on a Linux workstation. The relatively fast turnaround makes LATCH an

extremely useful code for vehicle design. The evolution of LATCH from a spherical/cylindrical system to a generalized body-fitted coordinate system enabled LATCH to use metric and inviscid streamline data from flow field solvers, like LAURA and DPLR and thus extend the applicability of the heating calculations to almost any vehicle geometry. The LATCH code has been shown to compare well with experimental, computational, and flight data^{20,21,22,23}.

In addition to surface heating rates, LATCH provides boundary layer edge data. LATCH computes the boundary layer thickness (δ) based on a momentum thickness (θ) and a shape-factor (δ/θ). LATCH calculates the momentum thickness, where as the shape-factor is a function of the wall to total enthalpy ratio. For conventional ground based facilities, where there is little spatial variation in wall enthalpy, this ratio is approximately constant. At flight conditions, the wall enthalpy varies; therefore, the shape-factor will vary both spatially over the vehicle surface and temporally through the trajectory. This behavior is illustrated in Figure 4, which shows the shape-factor from two LAURA solutions, one at Mach 6, the other at Mach 18, both on the STS-107 trajectory. The shape-factor is reduced with increasing Mach number. Over most of the windward surface the shape-factor is relatively constant; however, values increase as one moves laterally on the wing. In addition, at flight conditions enthalpy ratios are typically lower than values observed at ground test conditions. To approximate the effect of enthalpy ratio and shape-factor, the SABLE²⁴ boundary layer code computed the shape-factor as a function of enthalpy ratio using the ISSHVFW free stream conditions and assuming equilibrium flow. The data shown in Figure 5 was curve-fit and incorporated in LATCH. Also included on Figure 6 are viscous values from LAURA. Viscous values are roughly 13% below the LATCH values. While the shape-factor is insensitive to Mach number, there is an angle of attack effect that is not taken into account. However, the angle-of-attack is appropriate for most of the hypersonic trajectory since it remains near 40 degrees until approximately Mach 9.

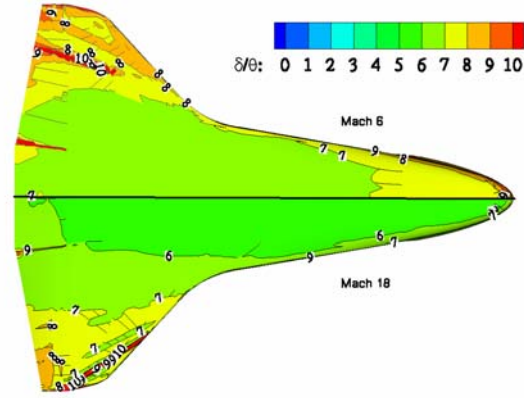


Figure 4. Shape-factor STS-107 $\alpha=40$

conditions. To approximate the effect of enthalpy ratio and shape-factor, the SABLE²⁴ boundary layer code computed the shape-factor as a function of enthalpy ratio using the ISSHVFW free stream conditions and assuming equilibrium flow. The data shown in Figure 5 was curve-fit and incorporated in LATCH. Also included on Figure 6 are viscous values from LAURA. Viscous values are roughly 13% below the LATCH values. While the shape-factor is insensitive to Mach number, there is an angle of attack effect that is not taken into account. However, the angle-of-attack is appropriate for most of the hypersonic trajectory since it remains near 40 degrees until approximately Mach 9.

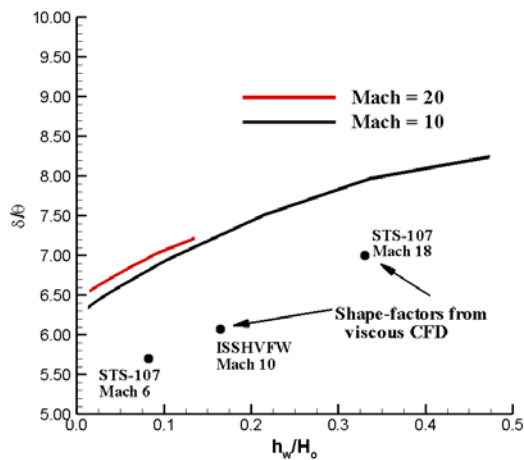


Figure 5. h_w/H_0 vs. δ/θ at $X/l = 0.3$ along Orbiter centerline at $\alpha=40$ degrees for equilibrium air flow.

B. LAURA

The Langley Aerothermodynamic Upwind Relaxation Algorithm (LAURA) is a computational fluid dynamics tool specialized for hypersonic re-entry flow that models the physics and chemistry associated with high temperature reacting gas flows in thermal equilibrium and non-equilibrium. LAURA is a three-dimensional, finite-volume, shock-capturing, structured grid solver that relaxes the full Navier-Stokes, thin-layer Navier-Stokes, or Euler equations in pseudo time to a steady state. Point-implicit relaxation is used at the start of the iterative process and as the converged state is approached, line-implicit relaxation is employed. The inviscid first-order flux is upwind biased using Roe's flux-difference splitting²⁵ with Harten's entropy fix²⁶ and is extended to second-order with Yee's Symmetric Total Variation Diminishing (STVD) approach²⁷. Viscous terms are approximated with second-order central differences. LAURA operates in a parallel (using MPI) computing environment and includes thermodynamic models for perfect gas²⁸, tetrafluormethane (CF_4), equilibrium air²⁹, or non-equilibrium³⁰ chemistry. For non-equilibrium flow, the thermodynamics and transport properties for each species are obtained from curve-fits as discussed in Ref. 30. The gas kinetic model is that of Park

as detailed in Ref. 31. LAURA simulates turbulent flow with a Baldwin-Lomax, Cebeci-Smith, or a two-equation $K-\omega$ model. No-slip conditions for velocity and temperature are applied at the wall. A coupled iterative procedure specifies the wall boundary temperature according to a radiation-equilibrium condition,

$$T_w^{n+1} = \eta (q^n / \varepsilon \sigma)^{0.25} + (1-\eta) T^n, \quad (1)$$

where q is the surface heat rate, ε is the surface emissivity, η is a relaxation factor (≈ 0.01), n is the solution iteration count, and σ is the Stefan-Boltzman constant.

C. DPLR

The Data Parallel Line Relaxation (DPLR) code, based on the work of Wright and Candler, solves the reacting Navier-Stokes equations including the effects of thermal non-equilibrium. DPLR is a parallel multi-block finite-volume code, valid in the hypersonic continuum flight regime, and computes 2-D, axisymmetric, and 3-D flows. The governing equations are implicitly advanced in time to a steady state by an efficient Gauss-Seidel line relaxation scheme. The inviscid fluxes are second-order based on a modified Steger-Warming flux splitting technique and extended to third-order accuracy using MUSCL extrapolation with a MIN-MOD flux limiter. Viscous fluxes use second-order central difference approximations. DPLR simulates turbulent flow with a compressible Baldwin-Lomax or shear stress transport (SST) model. At the wall, temperatures are constant (set by the user) or computed assuming a radiative equilibrium condition. Based on Park's 1990 work, a description of the chemical kinetic and two-temperature (T & T_v) thermal non-equilibrium model in DPLR is found in Ref. ³². The code contains several thermodynamic and transports models. The RTF work utilized a thermodynamic model based on equilibrium statistical mechanics. This model assumes the monatomic constituents of the gas mixture are point masses, and the diatomic constituents are rigid rotors/simple harmonic oscillators. The basis for the momentum transports is Blottner³³ curve fits for species viscosities and Wilke's³⁴ mixing rule. For energy transport, the Eucken relation for species thermal conductivities and Wilke's rule for the mixture are used. The reader is referred to Refs. [35 & 36] for further details regarding DPLR's capabilities and a comprehensive discussion on thermodynamic and transport models for RTF calculations.

IV. Analysis

This section describes the mesh index search algorithm, database interpolation methodology, and limitations of the BLPROP tool. Each subsection contains specific details to document the tool and allow an assessment of its strengths and weaknesses

A. Database Mesh Index Search Algorithm

As previously mentioned, database values reside at discrete coordinate points and these points form a mesh (in an order series) covering the Orbiter's windward surface. Each point in the mesh is referenced with an (I,J) index pair. Before database interpolation described in the next section can proceed, the database mesh index pair (I,J) nearest the damage location must be identified. Database coordinate locations and their associated (I,J) index pairs are identical for each solution in the database. Therefore, it is necessary to interrogate the database mesh only once to determine the (I,J) index pair nearest the damage location and not interrogate each database mesh individually. Prior to interpolation through the database, a simple geometric algorithm determines the mesh index pair nearest the input damage site. With this search methodology described below, there is no requirement for the damage location to be co-planar with the database surface. There is an allowance for some error in the specification of damage locations: damage locations need only be in the vicinity of the Orbiter surface and can lie above or below the database surface.

The algorithm that determines which (I,J) index pair is nearest the damage location uses angles between surfaces formed by the database mesh coordinates and the damage location to isolate the nearest index pair. Figure 6 graphically illustrates the surfaces listed below.

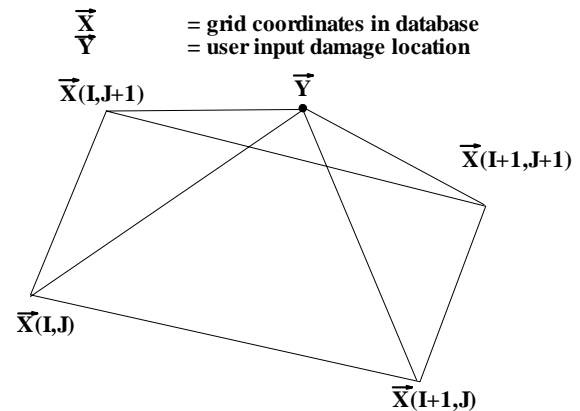


Figure 6. Database and damage coordinates

- Surface 1 = Defined by points $\bar{X}(I,J)$, $\bar{X}(I+1,J)$, $\bar{X}(I+1,J+1)$ and $\bar{X}(I,J+1)$
- Surface 2 = Defined by points $\bar{X}(I,J)$, $\bar{X}(I,J+1)$, and \bar{Y}
- Surface 3 = Defined by points $\bar{X}(I,J)$, $\bar{X}(I+1,J)$, and \bar{Y}
- Surface 4 = Defined by points $\bar{X}(I+1,J+1)$, $\bar{X}(I+1,J)$, and \bar{Y}
- Surface 5 = Defined by points $\bar{X}(I+1,J+1)$, $\bar{X}(I,J+1)$, and \bar{Y}

If the angle between surfaces 1 and 2, 1 and 3, 1 and 4, and 1 and 5 are all less than or equal to 90 degrees, the damage location resides within the normal projected volume of surface 1 and assigned to that corresponding (I,J) index pair. Special consideration exists for convex and concave surfaces (see Figure 7-8). For a concave surface, like that shown in Figure 7, projected volumes from multiple surfaces overlap and multiple (I,J) index pairs are identified for a single damage location. When this occurs, the index pair associated with the surface nearest the damage is used. Conversely, for a convex surface (see Figure 8), a damage location may reside between projected volumes: in this instance, an index pair is not found.

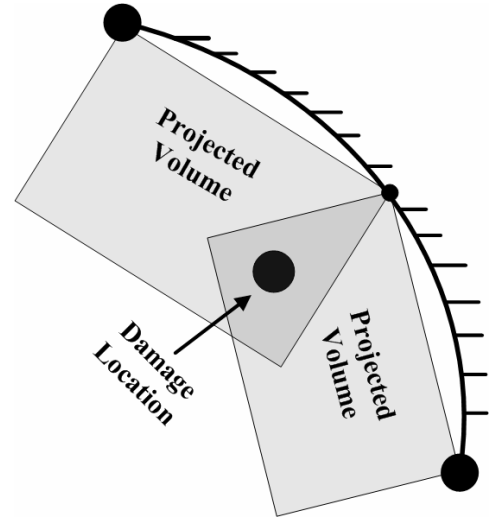


Figure 7. Concave condition

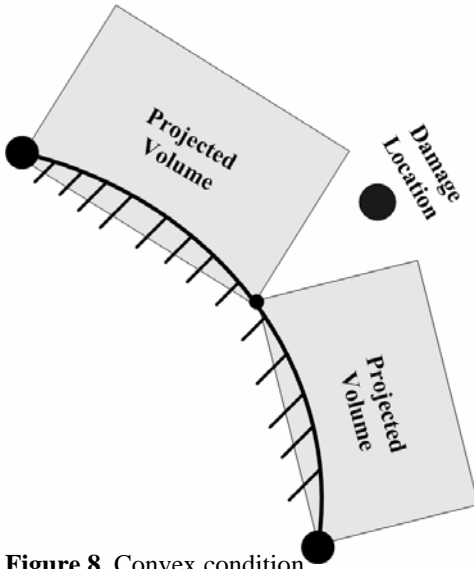


Figure 8. Convex condition

When this occurs, the search angle increases (from 90 degrees) in one-degree increments until an index is located. When interpolating for angle-of-attack and Mach number, database values at the (I,J) index pair are used. Spatially interpolation to the exact damage location is not necessary since the resolution of the database mesh is sufficient for the intended application.

B. Database Interpolation for input conditions

Knowing the database mesh index pair relative to the damage location, the BLPROP tool then interpolates for values at the input conditions. A first-order one-dimensional technique based on a Lagrange algorithm performs all interpolation. A non-dimensional normalization accounts for the difference between the database and input Reynolds number. Interpolated values at the user input angle-of-attack, as depicted in Figure 9, are determined across the Mach number range. Currently, values at the input condition are formed from the two database solutions that bound the input condition: replacement of this method with a technique that uses the entire range of points is planned. Before determining values at the input Mach number (see Figure 10), the interpolated values that reside at the input angle-of-attack are normalized using step-one of equation 2.

This process uses free stream reference values from Table 1 & 2. The two-step physics-based normalization is as follows:

		1 st step		2 nd step	
Pressure	→	$P_w/(\rho_\infty V_\infty^2)$		$P_w^*(\rho_\infty V_\infty^2)$	
Heating	→	q_w/q_{ref}		q_w^*/q_{ref}	(2)
$\delta, \theta, Re_\theta/M_e$	→	$(\delta, \theta, Re_\theta/M_e)/\sqrt{Re/ft}$		$(\delta, \theta, Re_\theta/M_e)^*\sqrt{Re/ft}$	
		evaluate w/ free stream = database conditions		evaluate w/ free stream = input conditions	

where q_{ref} is a Fay-Riddell prediction for stagnation heating rate on a 2.5-foot radius sphere. Normalization prior to Mach number interpolation partially accounts for the difference between the database and input Reynolds number. After performing the operations indicated in the 1st step of equation 2, values are interpolated at the input Mach

number. At this point, with the angle-of-attack and Mach number interpolation completed, the 2nd step in equation 2 is performed on the values residing at the input Mach number condition. This 2nd step uses free stream values at the input condition. The 2nd step in equation 2 completes the process of accounting for the difference between the database and input condition Reynolds number. The normalization indicated in equation 2 is appropriate for laminar attached perfect gas flow; however, even in the presence of gas chemistry it provides a reasonable approximation of Reynolds number influence.

BLPROP must be compiled such that all variables not specified as real*4 are promoted to double precision. When run on a 1.7GHz Pentium-4 workstation with Red Hat Linux using an Intel compiler, computing 14,600 damage locations required approximately 2 minutes. The BLPROP tool has run successfully when compiled using the Portland GroupTM and g95 compilers in a Linux environment and using the g95 compiler in a Windows environment. The code is structured such that data for multiple damage locations can be obtained at a single trajectory point or through an entire trajectory.

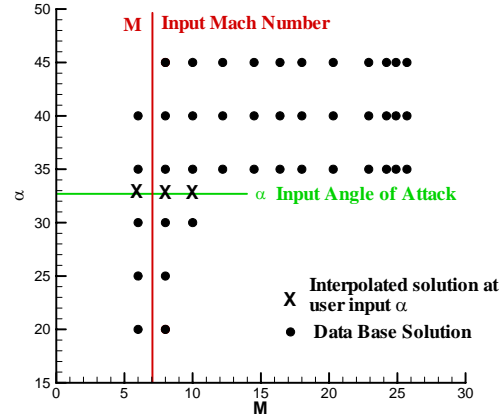


Figure 9. Angle-of-attack interpolation

C. BLPROP Limitations

- Hypersonic continuum flight regime only.
 - Mach number between 25.67 and 6
- Input Reynolds number within a factor of 3 of the database Reynolds number (empirically defined)
- BLPROP tool limited to shuttle’s windward surface
 - No data for small portion of shuttle nose cap
 - No data on wing leading edges
 - No data past body flap hinge line
- Surface heating-rate predicted at Mach 20.3 and below.
- Laminar flow
- BLPROP does not adjust interpolated values to account for database
 - Differences in chemistry model
 - viscous CFD non-equilibrium vs. LATCH equilibrium/perfect gas
 - Difference in surface catalysis
 - viscous CFD finite-catalytic vs. LATCH fully catalytic
 - Lack of viscous effects in LATCH data
- No extrapolation outside Mach number and angle-of-attack limits
- Free stream conditions must be within Mach Number, Reynolds number and angle-of-attack bounds

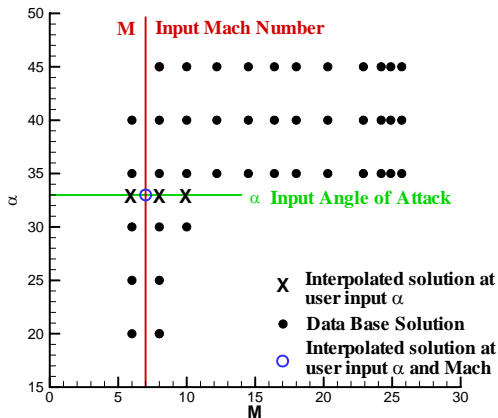


Figure 10. Mach number interpolation

V. Results

This section describes BLPROP algorithm verification, validation, and quantification of uncertainties. Addressing these areas was a requirement for Orbiter Configuration Control Board (OCCB) certification. OCCB certification is required for analysis tools used during Orbiter missions. It should be noted, the BLPROP tool is not a stand-alone tool, but is incorporated within the BLT and Cavity Heating tools; therefore, it did not independently go through the OCCB process. However, because it is integrated in the BLT and Cavity Heating tools and these tools required OCCB certification, BLPROP had similar verification, validation, and uncertainty quantification requirements. Definitions of verification and validation are those given in Ref. 37. Only boundary layer data relevant to the BLT and

Cavity Heating tools are presented in the subsections that follow.

A. BLPROP Verification

Verification addresses the question of fidelity of the conceptual model to the computational model: verification provides evidence that the model is solved right. It is not the purpose of verification to test components in terms of their applicability or appropriateness to a problem, but rather to make sure those components function and interact as the developer intended. The definition of verification found in Ref. 37 is as follows:

Verification: The process of determining that a model implementation accurately represents the developer’s conceptual description and specifications.

In addition to the use of write statements, compiler options, and user feedback to check for programming errors, there were two specific tests performed to verify the BLRPOP algorithm. For the first test, identical dummy database files containing a single constant value for each variable were loaded. Angle-of-attack and Mach number interpolation was performed, but non-dimensional normalization to account for Reynolds number was not. With these dummy files, this procedure, regardless of input conditions, returned the constant value in the dummy file, as it should. This test verified the coding for loading and handling of the database files and the coding of the interpolation routine. As a second test, BLPROP read in the actual database and interpolated at input conditions coincident with a solution in the database. A successful test should result in output that is identical to the coincident database solution. The t=1100 second condition at 40 degrees angle-of-attack listed in Table 2 was one of several conditions tested. The flooded contours in Figure 11 illustrate the results of this second test. Red and black contour lines from the interpolated and coincident database solution are shown, respectively. The variables in the figures are boundary layer thickness, momentum thickness, transition parameter, and edge Mach number. The overlapping contour lines indicate the solutions are nearly identical. When performed at other conditions, this test yielded results similar to those shown; therefore, additional results are not presented. While verification is a never-ending process, based on the above results the BLPROP algorithm is functioning as intended.

B. BLPROP Validation and Uncertainties

Validation provides evidence that the right model is solved: it addresses the question of the fidelity of the model to specific real world conditions. The definition of validation found in Ref. 37 is as follows:

Validation: The process of determining the degree to which a model is an accurate representation of the real-world from the perspective of the intended uses of the model.

Validation of a computational model usually takes the form of comparing computed against “real-world” results, like experimental data. However, in the context of this paper solutions from a solver used to create the database are interpreted as “real-world”. Results from the BLPROP algorithm are limited by the database and the best BLPROP can do is reproduce a database solution. In light of this limitation, comparing interpolated data with computed data from LAURA, DPLR, or LATCH is appropriate for validation.

Table 3. Non-coincident free stream values used for comparison with BLPROP tool

Case	Mission	Mach	Solver	T_∞ [R]	α [deg]	V_∞ [ft/s]	ρ_∞ [slug/ft ³]	Difference from Database Free Stream		
								Mach	α	% Δ Reynolds/ft
1	STS-88	7.17	LATCH	473	32.50	7643	3.711×10^{-6}	1.15	2.50	16
2	STS-2	14.23	LATCH	465	42.50	15068	7.382×10^{-7}	0.27	2.50	36
3	STS-114	25.67	LAURA	367	39.97	24177	7.266×10^{-8}	0.00	0.10	130
4	STS-2	24.30	DPLR	363	39.40	22703	1.115×10^{-8}	0.10	0.60	26

If the BLPROP model accurately represented the “real-world”, interpolated data from BLPROP would be equivalent to data computed by a method used to build the computational database. The BLPROP algorithm will be validated using this methodology: by comparing computed to interpolated data. The interpolated data is generated in the fashion of a “real-world” application of BLPROP. In a “real-world” application, damage location and free stream conditions are input to BLPROP, and boundary layer data are output. For validation, LAURA, DPLR, and

LATCH predicted boundary layer data at free stream conditions not coincident with those used to construct the BLPROP database. Non-coincident free stream conditions were taken from previous Orbiter flights. Table 3 lists the non-coincident free stream conditions, computational solver, their variation from the database conditions, and the corresponding STS mission identifier. When exercised for pre-mission and on-mission analyses, the input trajectory, most likely, will not correspond to either the ISSHVFW or STS-107. Using non-coincident input values is a rigorous test and is a real world application of the BLPROP algorithm.

Once computed, solutions from LAURA, DPLR, and LATCH were processed in the same fashion as solutions used to build the BLPROP database. Specifically, the non-coincident solutions were interpolated to the database mesh using Tecplot. This minimized the influence of Tecplot interpolation on the comparisons of computed and interpolated results, since all results were subject to Tecplot interpolation. Non-coincident solutions and solutions upon which the database was based were computed on the same computational mesh. LAURA computed inviscid solutions on a grid comprised of 153 stream wise points, 193 circumferential points, and 49 points between the body and inflow boundary. When computing viscous solutions, LAURA and DPLR used grids developed for RTF computational activities. The baseline viscous grid contained approximately 1 million cells, with 64 cells between the body and inflow boundary. Further details regarding the RTF grids are in Ref. 35.

Shown in Figure 12-15 are percentage differences between interpolated and computed values. Boundary layer edge thickness, momentum thickness, transition parameter (Re_{θ}/M_e), and edge Mach number are presented for each case in Table 3. All figures share the same color scale and value range ($\pm 25\%$). Generally speaking, percentage differences are lowest between the interpolated and LATCH data: the agreement is within $\pm 5\%$ for all values shown. Percentage differences between interpolated and viscous CFD are slightly higher: over the majority of the vehicle agreement is within $\pm 10\%$ for both cases 3 and 4. (The percent difference for edge Mach number is within $\pm 5\%$). Higher differences exist forward and on the outboard and trailing edges of the wing for case 3. Case 3 has the largest change in Reynolds number, over a factor of two. The non-dimensional normalization affects all values shown, except for the edge Mach number, and is the likely cause of the deterioration in performance. While the current scaling produces reasonable agreement for moderate changes in Reynolds number, a compressible based scaling may be more appropriate for a large change in Reynolds number.

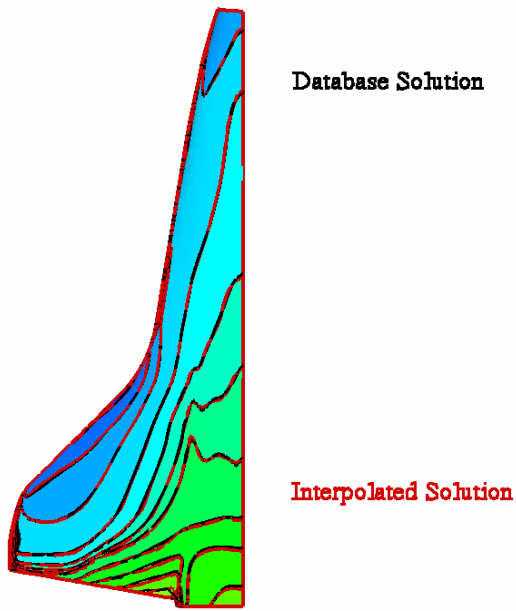
The percentages quoted above address differences between interpolation and computation. The inherent uncertainty in the computational solutions that form the database is not included. Based on comparison with the viscous data, uncertainty between the BLPROP tool and the “real-world” is approximately $\pm 10\%$. This level of uncertainty is below the expected range of the analysis tools BLPROP supports.

VI. Summary

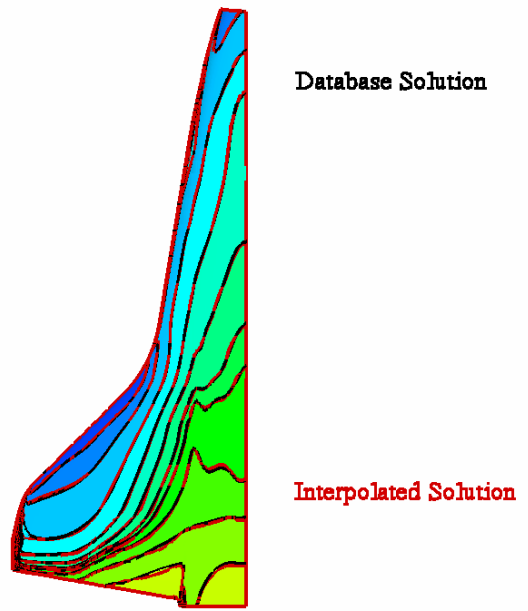
This paper describes a new interpolation tool that automates the process of obtaining boundary layer edge data that is input to the BLT and Cavity Heating tools. The BLPROP tool computes boundary layer edge values spatially on the windward Shuttle Orbiter surface and temporally along an Orbiter trajectory. To cover the hypersonic continuum flight regime, 42 solutions were computed with a two-layer and benchmark CFD solvers. The BLPROP algorithm uses one-dimensional first-order Lagrange interpolation to produce values at the input angle of attack and Mach number. A non-dimensional normalization accounts for the difference between the database and input Reynolds numbers. Traditional means of checking for programming errors and two specific tests were successful in verifying the algorithm. The code was exercised as intended to be used during missions. Results from these exercises compared with computed data help validate the algorithm and establish uncertainty levels. Based on observed percent differences, the uncertainty in BLPROP values is approximately $\pm 10\%$ and this is within the level required by supported analysis tools.

VII. Acknowledgements

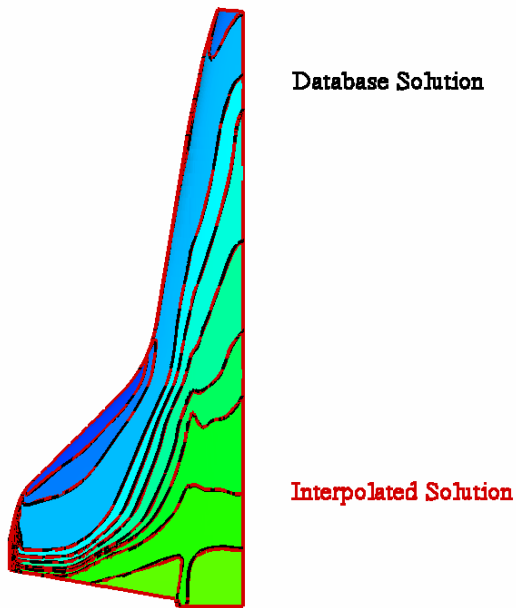
The authors would like to thank James Reuther from NASA Ames Research Center for providing the DPLR boundary layer edge data used in the database and David Saunders from ELORET for the providing boundary layer edge definition algorithm, BLAYER_RESULTS. In addition, the authors thank Gerald Kinder from Boeing for providing the Orbiter entry trajectories.



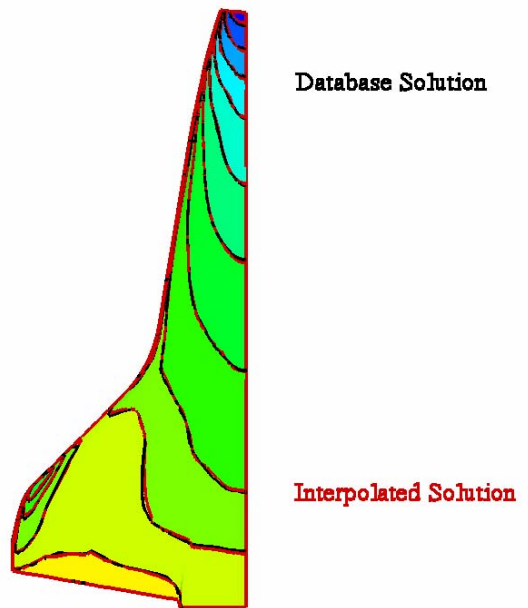
(a) boundary layer edge thickness



(c) transition parameter



(b) momentum thickness



(d) edge Mach number

Figure 11. Comparison at conditions coincident with database, $M=12.20$, $\alpha=40.00$, ISSHVFVW

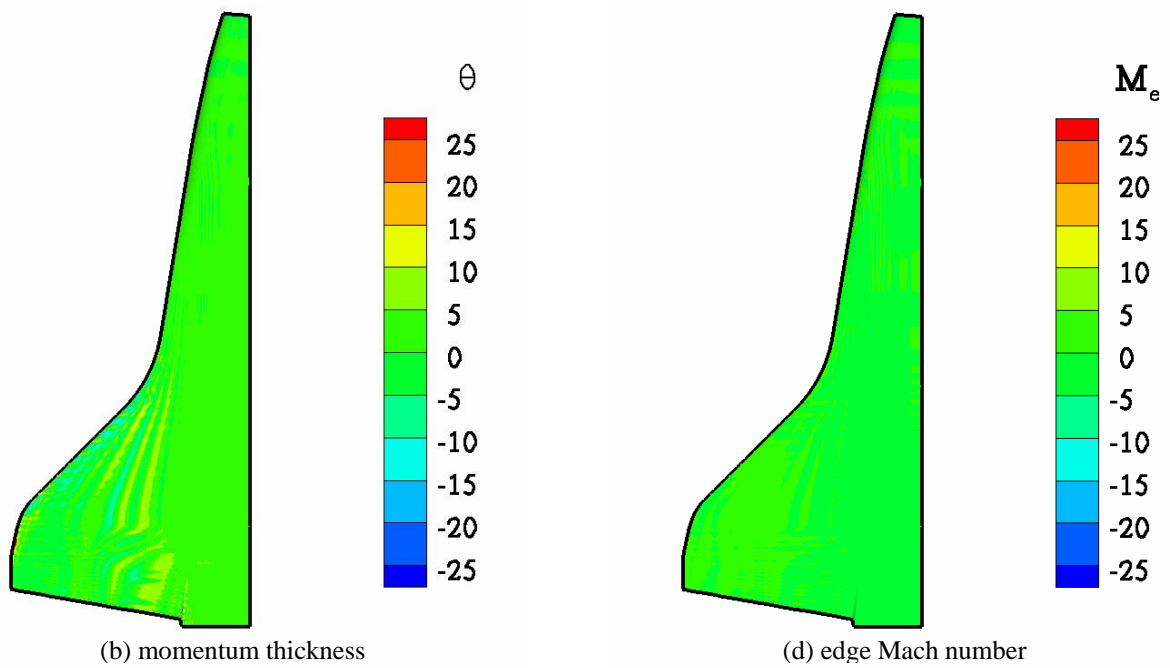
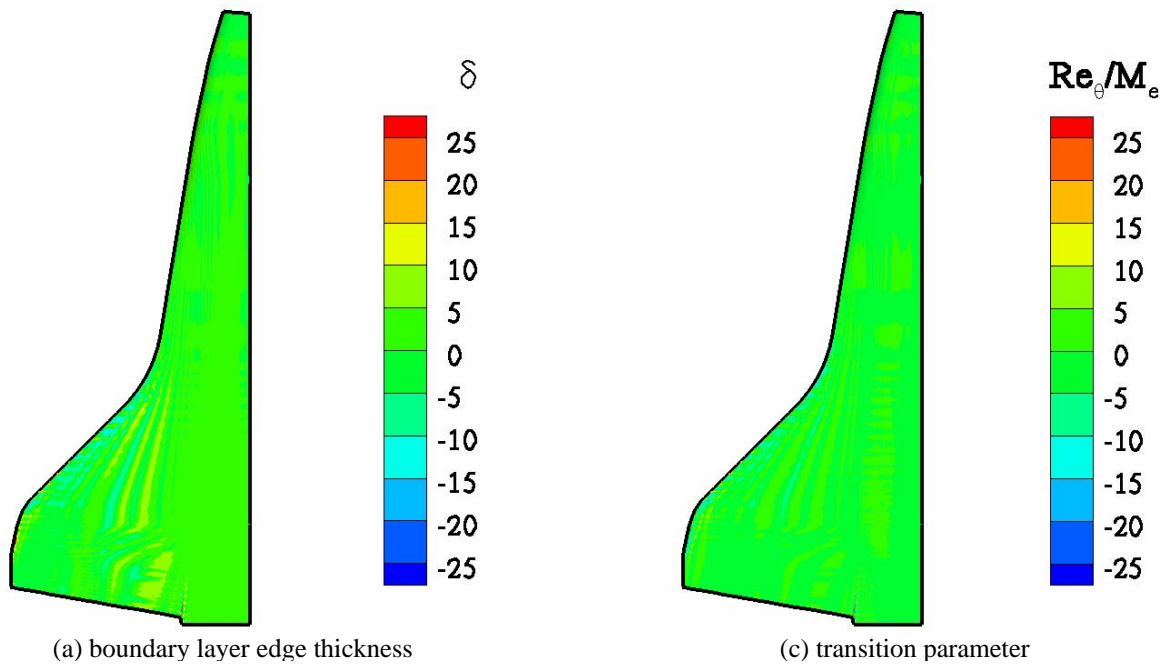


**Figure 12. Case 1 – Percentage difference between interpolated and computed values.
(Computed values from LAURA + LATCH)**

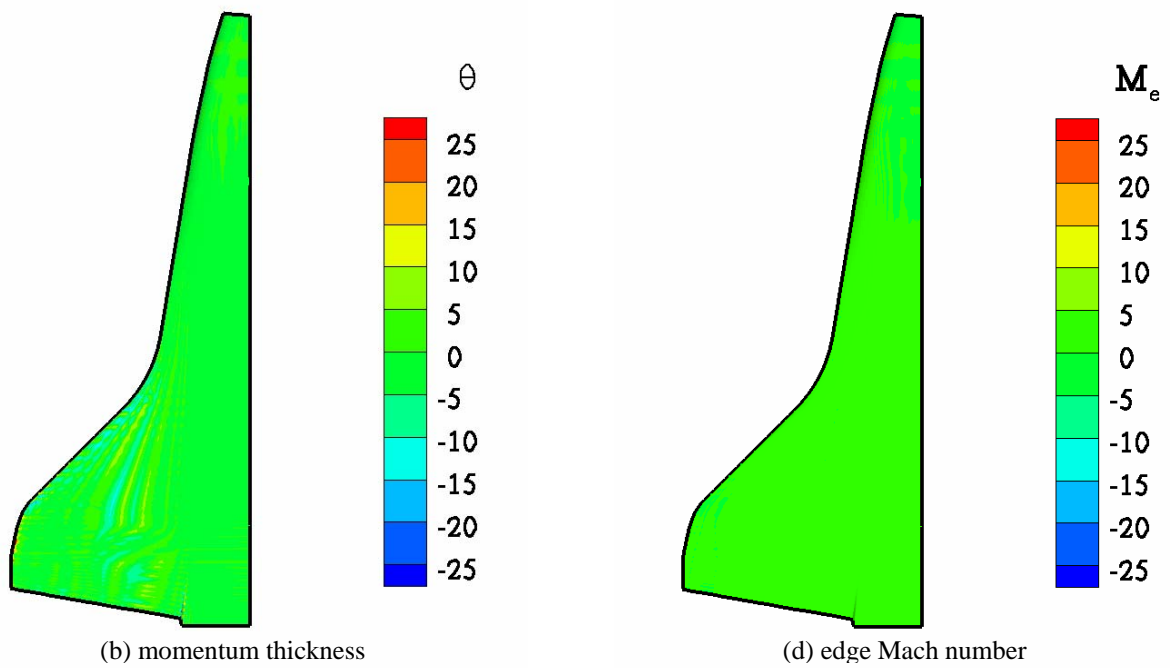
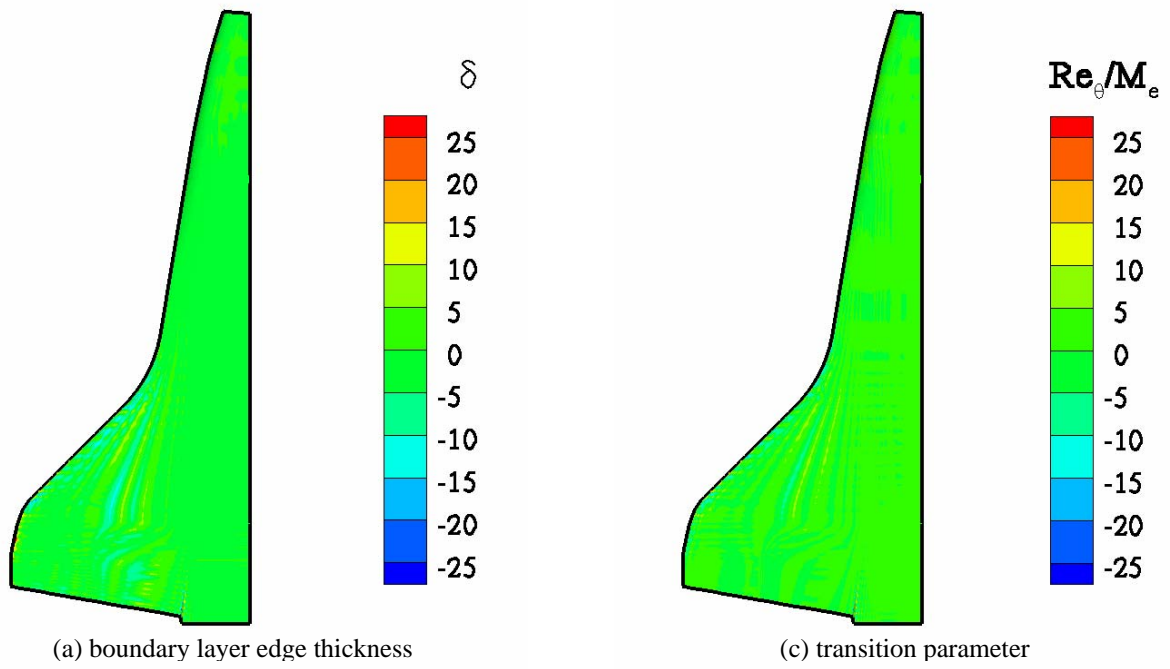


**Figure 13. Case 2 - Percentage difference between interpolated and computed values.
(Computed values from LAURA + LATCH)**

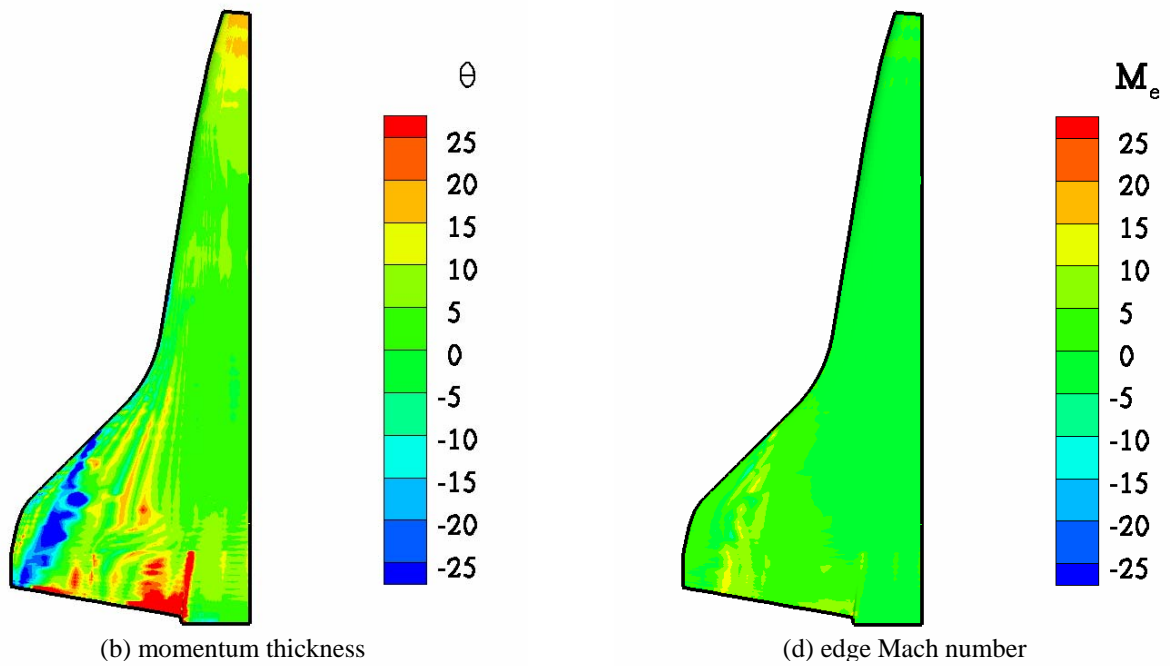
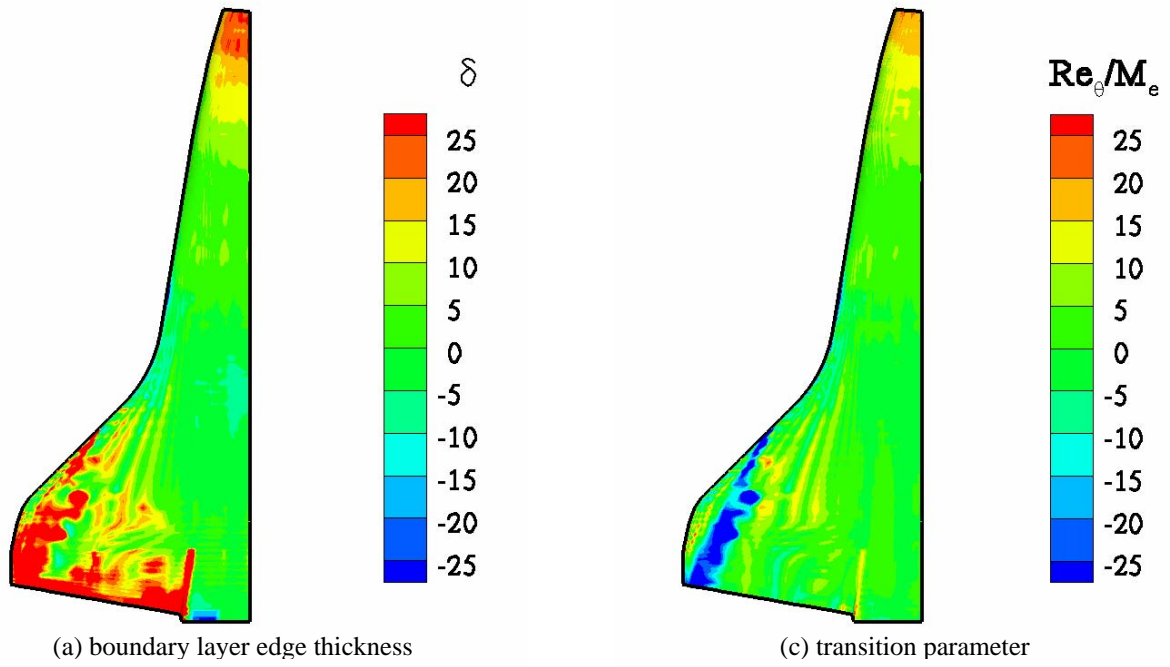


**Figure 14. Case 3 - Percentage difference between interpolated and computed values.
(Computed values from LAURA)**

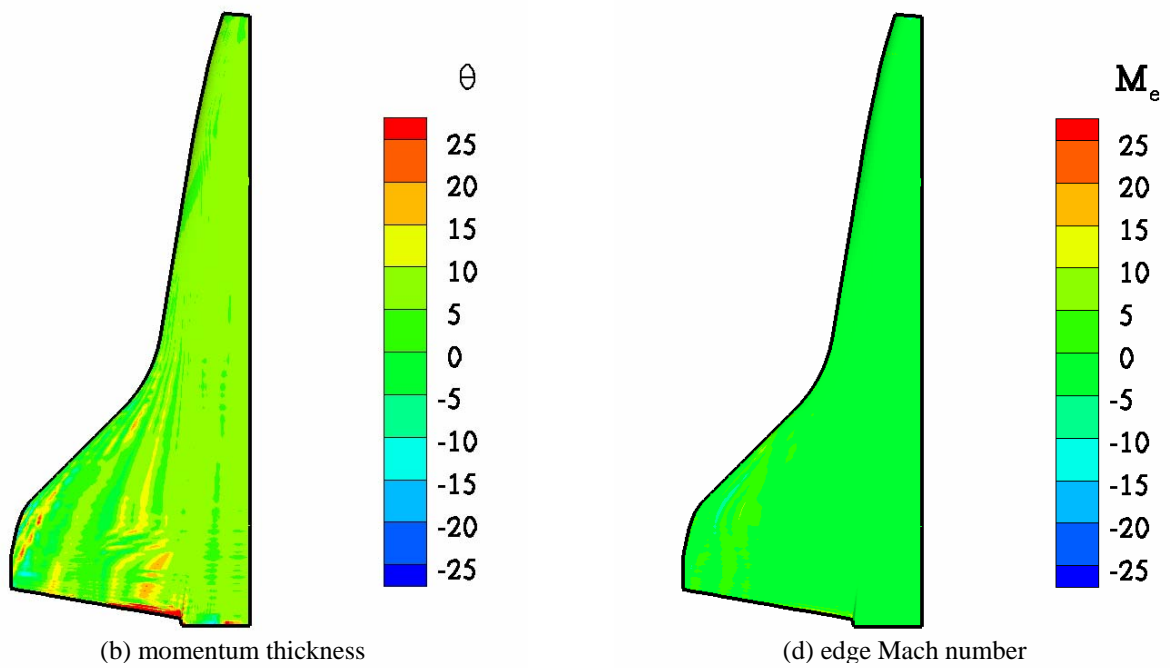
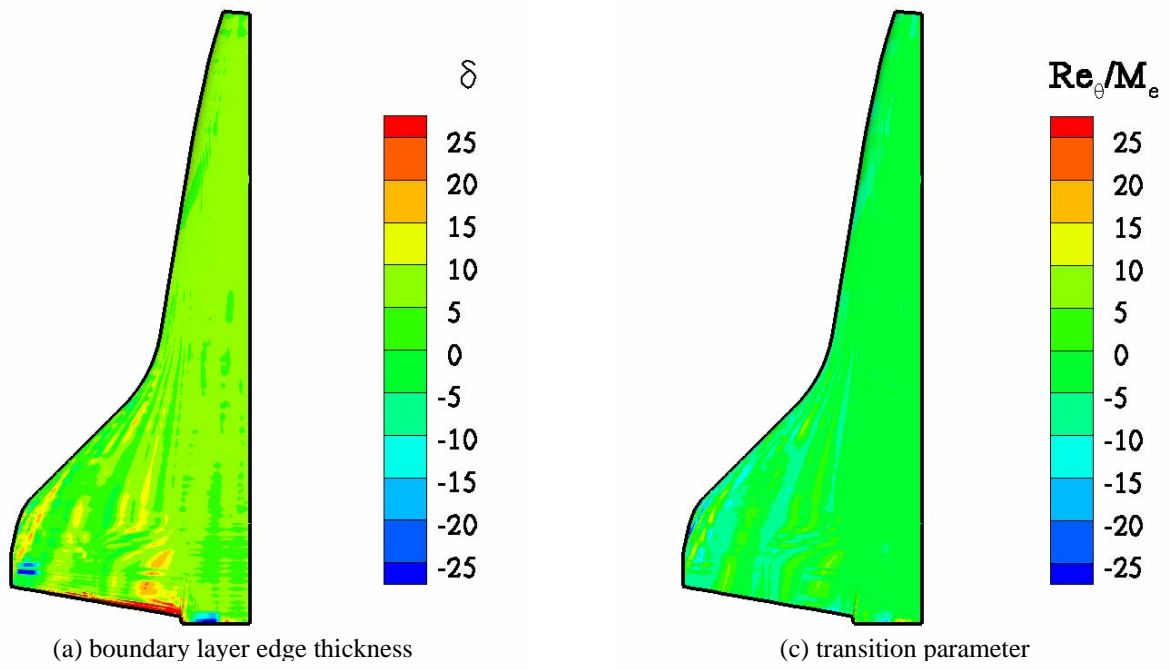


**Figure 15. Case 4 - Percentage difference between interpolated and computed values.
(Computed values from DPLR)**

-
- ¹ Campbell, C. H., Bourland, G., Bouslog, S. A., Horvath, T. J., Berry, S. A., Gnoffo, P. A., Reuther, J., Chao, D., Anderson, B., and Picetti, D., "Orbiter Return-To-Flight Entry Aeroheating," AIAA Paper 2006-2917, June 2006
- ² Columbia Accident Investigation Board Report, Report Volume 1, August 2003
- ³ Horvath, T. J., Berry, S. A., Merski, N. R., Berger, K. T., Liechty, D. S., and Schneider, S. P., "Disposition of Shuttle Thermal Protection System Damage / Repair From the Perspective of Hypersonic Boundary Layer Transition," AIAA Paper 2006-2919, June 2006
- ⁴ Berry, S. A.; and Hamilton, H. H.: "Discrete Roughness Effects on Shuttle Orbiter at Mach 6," AIAA Paper 2002-2744, June 2002.
- ⁵ Berry, S. A., Horvath, T. J., Hollis, B. R., Thompson, R. A., and Hamilton, H. H., "X-33 Hypersonic Boundary Layer Transition," *Journal of Spacecraft and Rockets*, Vol. 38, No. 5, 2001, pp. 646-657 (see also AIAA Paper 99-3560, June 1999).
- ⁶ Horvath, T. J., Berry, S. A., Merski, N. R., Fitzgerald, S. M., "X-38 Experimental Aerothermodynamics," AIAA Paper 2000-2685, June 2000.
- ⁷ Berry, S.A., Horvath, T.J., Greene, F.A., Kinder, G., and Wang, K.C., "Overview of Boundary Layer Transition Research in Support of Orbiter Return To Flight," AIAA Paper 2006-2918, June 2006
- ⁸ Berry, S. A., Fischer-Cassady, A., Kirk, B., Wang, K.C., and Hyatt, A., "Boundary Layer Transition Results From STS-114," AIAA Paper 2006-2922, June 2006
- ⁹ McGinley, K., Berry, S.A., Kinder, G., Barnwell, M., Wang, K.C., and Kirk, B., "Review of Orbiter Flight Boundary Layer Transition Data," AIAA Paper 2006-2921, June 2006.
- ¹⁰ Cheatwood, F. M., and Gnoffo, P. A., "User's Manual for the Langley Aerothermodynamic Upwind Relaxation Algorithm," NASA TM-4674, April 1996.
- ¹¹ Wright, M. J., Candler, G. V., and Bose, D., "Data-Parallel Line Relaxation Method for the Navier-Stokes Equations," *AIAA Journal*, Vol 36., No. 9., 1998, pp1603-1609.
- ¹² Hamilton II, H. H., DeJarnette, F. R., and Weilmuenster, K. J., "Application of Axisymmetric Analog for Calculating Heating in Three-Dimensional Flows," *Journal of Spacecraft and Rockets*, Vol. 24, Jul.-Aug. 1987, pp. 296-302.
- ¹³ Private communication, Saunders, D., ELORET Corporation
- ¹⁴ Private Communication, Kinder, G., Boeing Corporation
- ¹⁵ Shuttle Operational Data Book, <https://opo.jsc.nasa.gov/sodw/> NSTS-08934
- ¹⁶ Hamilton II, H. H., DeJarnette, F. R., and Weilmuenster, K. J., "Application of Axisymmetric Analog for Calculating Heating in Three-Dimensional Flows," *Journal of Spacecraft and Rockets*, Vol. 24, Jul.-Aug. 1987, pp. 296-302.
- ¹⁷ Hamilton II, H. H., Greene, F. A., and DeJarnette, F. R., "Approximate Method for Calculating Heating Rates on Three-Dimensional Vehicles," *Journal of Spacecraft and Rockets*, Vol. 31, No. 3, May-Jun 1994, pp. 345-354.
- ¹⁸ Cook, J. C., "An Axially Symmetric Analogue for General Three-Dimensional Boundary Layers," Reports and Memoranda 3200, 1961
- ¹⁹ Zoby, E. V., Moss, J. N., and Sutton, K., "Approximate Convective Heating Analysis for Hypersonic Flows," *Journal of Spacecraft and Rockets*, Vol. 18, No. 1, 1981 pp. 64-70.
- ²⁰ Micol, J., "Aerothermodynamic Measurement and Prediction for a Modified Orbiter at Mach 6 and 10," AIAA Paper 91-1436, June 1991.
- ²¹ Throckmorton, D. A., and Hartung, L. C., "Space Shuttle Entry Heating Data Book," Vol. I-STS2, NASA RP-1191, May 1988.
- ²² Riley, C. J., Kleb, W. L., and Alter, S. J., "Aeroheating Predictions for X-34 Using an Inviscid-Boundary Layer Method," AIAA Paper 98-0880, Jan. 1998.
- ²³ Hamilton II, H. H., Greene, F. A., and Weilmuenster, K. J., "Comparison of Heating Calculations with Experimental Data on a Modified Shuttle Orbiter," *Journal of Spacecraft and Rockets*, Vol. 29, No. 2, 1992, pp. 208-215.
- ²⁴ Hamilton II, H. H., Millman, D. R., and Greendyke, R. B., "Finite-Difference Solution for Laminar or Turbulent Boundary Layer Flow Over Axisymmetric Bodies With Ideal Gas, CF_4 , or Equilibrium Air Chemistry," NASA TP-3271, Dec. 1992.
- ²⁵ Roe, P. L., "Approximate Riemann Solvers, Parameters Vectors, and Difference Schemes," *Journal of Computational Physics*, Vol. 43, No. 2, 1981, pp. 357-372.
- ²⁶ Harten, A., "High Resolution Schemes for Hyperbolic Conservation Laws," *Journal of Computational Physics*, Vol. 49, No. 3, 1983, pp. 357-393.
- ²⁷ Yee, H. C., "On Symmetric and Upwind TVD Schemes," NASA TM-86842, September 1985.
- ²⁸ Gnoffo, P. A., "An Upwind-Biased, Point-Implicit Relaxation Algorithm for Viscous Compressible Perfect-Gas Flows," NASA TP-2953, 1990.
- ²⁹ Greene, F. A., and Gupta, R. N., "Viscous Equilibrium Computations Using Program LARUA," *Journal of Spacecraft and Rockets*, Vol. 29, No. 5, 1992, pp.627-632.
- ³⁰ Gnoffo, P. A., Gupta, R. N., and Shinn, J. L., "Conservation Equations and Physical Models for Hypersonic Air Flows in Thermal and Chemical Nonequilibrium," NASA TP-2867.
- ³¹ Park, C., "Review of Chemical-Kinetic Problems of Future NASA Missions, I: Earth Entries," *JTHT*, 7(3), pp. 385-398, July 1993
- ³² Park, C, Nonequilibrium Hypersonic Aerothermodynamics, John Wiley, New York, 1990.
- ³³ Blottner, F G, Johnson, M, and Ellis, M, "Chemically Reacting Viscous Flow Program for Multi-Component Gas Mixtures," Report SC-RR-70-754, Sandia Laboratories, Albuquerque, NM, 1971.
- ³⁴ Wilke, C R, "A Viscosity Equation for Gas Mixtures," *J. Chemical Physics*, Vol. 18, 1950, pp. 517-519.
- ³⁵ Reuther, J J, Brown, J L, Prabhu, D K, McDaniel, R D, Saunders, D A, and Palmer, G E, "External Computational Aerothermodynamic Analysis of the Space Shuttle Orbiter at STS-107 Flight Conditions," AIAA Paper No. 2004-2281, 37th AIAA Thermophysics Conference, Portland, OR, June 2004.
- ³⁶ Reuther, J J, Prabhu, D K, Wright, M J, Brown, J L, and Saunders, D A, "Computational Fluid Dynamics for Winged Re-entry Vehicles at Hypersonic Conditions," AIAA Paper No. 2004-2537, 34th AIAA Fluid Dynamics Conference, June 2004.
- ³⁷ Oberkampf, W. L., Sindir, M. M., and Conlisk, A. T., Guide for the Verification and Validation of Computational Fluid Dynamics Simulations, AIAA G-077-98, 1998